J. Phys. B: Atom. Molec. Phys., Vol. 9, No. 4, 1976. Printed in Great Britain. ©1976

The 1s–2s and 1s–2p excitation of atomic hydrogen by electron impact

A E Kingston, W C Fon† and P G Burke

Department of Applied Mathematics and Theoretical Physics, Queen's University, Belfast, N Ireland

Received 13 October 1975

Abstract. The $1s \rightarrow 2s$ and $1s \rightarrow 2p$ total and differential cross sections for electron impact excitation of atomic hydrogen are calculated from 13 eV to 300 eV. The 1s–2s–2p close-coupling approximation is used for the low partial waves and the unitarized Born approximation for the high partial waves. At the highest energy up to 500 partial waves are included. The calculated differential cross sections are in quite good agreement with the measurements of Williams and Willis.

1. Introduction

The excitation of ground-state hydrogen atoms to the $n = 2$ states by electron impact is of fundamental interest. From the theoretical point of view, atomic hydrogen is the only target for which the atomic states are known exactly. Consequently the collision problem is not complicated by atomic structure problems. Experimentally it is important because of the many applications in which these cross sections play a fundamental role.

These cross sections have been reviewed by Moiseiwitsch and Smith (1968) and Williams and Willis (1974). They show that below about 50 eV significant differences exist between the calculated total cross sections for the $n = 2$ states and the relative measurements normalized to the Born approximation at high energies. It is thus of very great importance to have accurate calculations at intermediate and high energies to provide a normalization for experiments. Very recently Williams and Willis (1975) have obtained absolute differential cross sections in the energy range from 54 to 680 eV, which are unaffected by cascade effects. It is therefore of interest to obtain accurate theoretical differential cross sections to compare with this work.

At present there is considerable disagreement between the calculated differential cross sections and the measurements of Williams and Willis (1975) which agree to within experimental accuracy with the relative angular distributions of Williams (1969) at all energies and at angles greater than 30°. This disagreement between theory

† On sabbatical leave from the Department of Mathematics, University of Malaya, Kuala Lumpur, Malaysia.

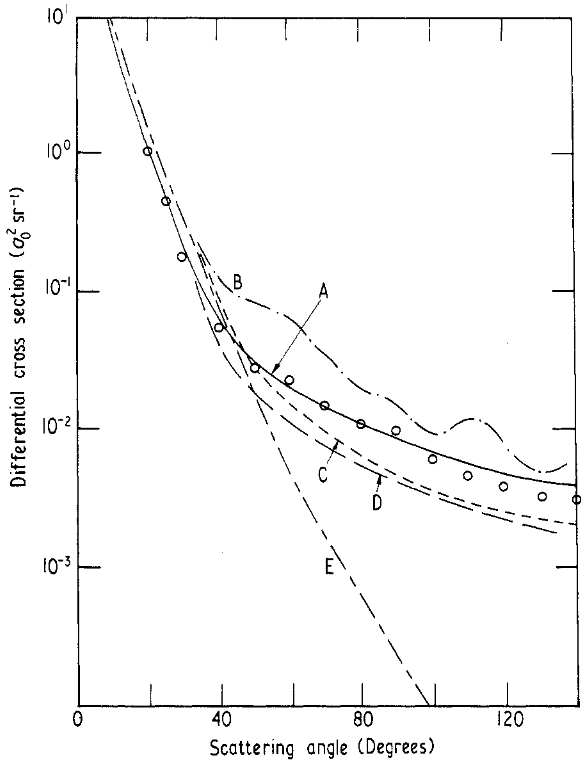

Figure 1. Differential cross section for the process e + H(1s) ⟶ e + H(2s + 2p) at 54·4 eV. A, present 1s–2s–2p close-coupling calculation; B, 1s–2s–2p close-coupling calculation (Scott 1965); C, second-order potential calculations (Bransden *et al* 1972); D, Glauber approximation (Ghosh and Sil 1970); E, first Born approximation. ○, Experimental data (Williams and Willis 1975).

and experiment at 54 eV is shown in figure 1, where we plot results from (i) the first Born approximation, (ii) the Glauber approximation (Ghosh and Sil 1970), (iii) the 1s–2s–2p three-state close-coupling approximation (Scott 1965) and (iv) the second-order potential approximation (Bransden *et al* 1972). Calculations using the distorted wave approximation (Shelton *et al* 1971), the Coulomb-projected Born approximation (Geltman and Hidalgo 1971) and the distorted wave polarized orbital method (McDowell *et al* 1975) are also discussed by Williams and Willis (1975).

In this paper we use the 1s–2s–2p close-coupling approximation (Burke *et al* 1963) to calculate the low partial waves and the unitarized Born approximation (Lawson *et al* 1961) to calculate the high partial waves. We find that the close-coupling *T*-matrix elements tend to the unitarized Born results as the angular momentum becomes large for all elements which contribute to the excitation of the $n = 2$ states. Thus our results may be regarded as accurate estimates of the complete three-state close-coupling approximation. We argue that as the energy becomes large the three-state close-coupling approximation rapidly approaches the exact result since it contains the dominant long-range r^{-2} potentials which affect the 1s ⟶ 2s and 1s ⟶ 2p excitation cross sections. Thus we believe that our calculations provide an accurate standard above about 100 eV, against which other calculations can be judged.

2. Theory and numerical calculations

The close-coupling approximation is well known and has been described by many authors (e.g. Burke and Schey 1962, Burke and Smith 1962). We shall only present the basic formulae for the scattering amplitude and cross section here.

The wavefunction describing an electron incident on an atom in state ϕ_i and scattered leaving the atom in any state ϕ_j is

$$\Psi \underset{r\to\infty}{\sim} \phi_i \chi_{1/2}^{m_i} \mathrm{e}^{\mathrm{i}k_i z} + \sum_j \phi_j \chi_{1/2}^{m_j} f_{ij}(\theta) \frac{\mathrm{e}^{\mathrm{i}k_j r}}{r} \tag{1}$$

where $\chi_{1/2}^{m_i}$ is the spin function for the scattered electron and where the wavenumber k_i is related to the total energy of the system E and the energy of the atomic state E_i through

$$E = E_i + \tfrac{1}{2}k_i^2. \tag{2}$$

The scattering amplitude is given (Burke 1971, Moores 1971) by

$$f_{ij}(\theta, \phi) = -\mathrm{i}\left(\frac{\pi}{k_i k_j}\right)^{1/2} \sum_{LSl_il_j} \mathrm{i}^{(l_i-l_j)}(2l_i+1)^{1/2} C_{L_il_i}(LM_L; M_{L_i}0) C_{S_i 1/2}(SM_S; M_{S_i}m_i)$$
$$\times\, C_{L_jl_j}(LM_L; M_{L_j}m_{l_j}) C_{S_j 1/2}(SM_S; M_{S_j}m_j) T_{ij} Y_{l_j}^{m_{l_j}}(\theta, \phi). \tag{3}$$

The differential cross section is given by

$$\frac{\mathrm{d}\sigma_{ij}(\theta,\phi)}{\mathrm{d}\Omega} = \frac{k_j}{k_i}|f_{ij}(\theta,\phi)|^2. \tag{4}$$

The total cross section for the transition $\alpha_i L_i S_i \to \alpha_j L_j S_j$ is obtained by integrating equation (3) over all angles averaging over initial spin directions and summing over final spin directions:

$$\sigma(\alpha_i L_i S_i \to \alpha_j L_j S_j) = \frac{\pi}{k_i^2} \sum_{LSl_il_j} \frac{(2L+1)(2S+1)}{2(2L_i+1)(2S_i+1)} |T_{ij}|^2. \tag{5}$$

For specified spin S and excitation from ground state ($l_i = 0$) equation (3) can be written as

$$f_{ij}^S = -\mathrm{i}\left(\frac{\pi}{k_i k_j}\right)^{1/2} \sum_{Ll_j} \mathrm{i}^{L-l_j}(2L+1) C_{L_jl_j}(L0, M_{L_j} - M_{L_j}) Y_{l_j}^{-M_{L_j}} T_{ij}^{SL}. \tag{6}$$

In the case of an e–H system, $S = 0$ or 1. The relation between the T matrix and the R matrix is given by the matrix equation

$$\mathbf{T} = \frac{2\mathrm{i}\mathbf{R}}{\mathbf{1} - \mathrm{i}\mathbf{R}}. \tag{7}$$

All the quantities in formulae (3) to (7) are defined by Burke (1971) and Moores (1971).

R-matrix elements for $0 \leqslant L < L_{\mathrm{cc}}$ are obtained by the close-coupling approximation with exchange. For $L_{\mathrm{cc}} \leqslant L < L_{\mathrm{cc}}^{\mathrm{NE}}$ they are obtained by close-coupling without exchange. For $L_{\mathrm{cc}}^{\mathrm{NE}} \leqslant L \leqslant L_{\max}$ they are obtained by the Born approximation. The values of $L_{\mathrm{cc}}, L_{\mathrm{cc}}^{\mathrm{NE}}$ and $L_{\max}$ used in the final calculation are displayed in table 1.

Table 1. Method used to calculate R matrices used in the present calculations (see text for explanation).

Energy of incident electron (Ryd)	L_{cc}	L_{cc}^{NE}	L_{max}
1·0	6	17	100
1·44	7	19	100
2·25	7	22	100
4·0	8	26	150
7·354	8	28	250
10·0	8	28	300
14·708	8	28	400
22·062	8	28	500

At very large values of L the Born approximation calculations were simplified greatly by using the following asymptotic forms in the Born reactance matrices:

$$R^L_{1sL,2pL+1} = \frac{64\pi}{243}\left(\frac{2(L+1)}{2L+1}\right)^{1/2}\left(\frac{k_2}{k_1}\right)^{L+3/2}\frac{\Gamma(L+1)}{\Gamma(\frac{1}{2})\Gamma(L+\frac{5}{2})}$$
$$\times\left[1+\sum_{n=1}^{\infty}\left(\frac{k_2}{k_1}\right)^{2n}\prod_{j=1}^{n}\frac{(L+j)(j-\frac{1}{2})}{j(L+\frac{3}{2}+j)}\right] \tag{8}$$

$$R^L_{1sL,2pL-1} = \frac{-64\pi}{243}\left(\frac{2L}{2L+1}\right)^{1/2}\left(\frac{k_2}{k_1}\right)^{L-1/2}\frac{\Gamma(L)}{\Gamma(\frac{3}{2})\Gamma(L+\frac{1}{2})}$$
$$\times\left[1+\sum_{n=1}^{\infty}\left(\frac{k_2}{k_1}\right)^{2n}\prod_{j=1}^{n}\frac{(L+j-1)(j-\frac{3}{2})}{j(L+j-\frac{1}{2})}\right] \tag{9}$$

$$R^L_{2sL,2pL+1} = -\frac{3}{(L+1)}\left(\frac{L+1}{2L+1}\right)^{1/2} \tag{10}$$

$$R^L_{2sL,2pL-1} = \frac{3}{L}\left(\frac{L}{2L+1}\right)^{1/2} \tag{11}$$

$$R^L_{2pL+1,2pL+1} = -\frac{6k_2}{(2L+1)(L+1)} \tag{12}$$

$$R^L_{2pL+1,2pL-1} = \frac{6k_2}{(2L+1)}\left(\frac{1}{L(L+1)}\right)^{1/2} \tag{13}$$

$$R^L_{2pL-1,2pL-1} = -\frac{6k_2}{L(2L+1)}. \tag{14}$$

The R-matrix elements calculated from the Born approximation $R^L_{1sL,1sL}$, $R^L_{1sL,2sL}$ and $R^L_{2sL,2sL}$ are found to be very small when compared with other R-matrix elements for large L in the energy range considered in this paper.

These asymptotic formulae for the Born reactance matrix elements are derived using only the long-range r^{-n} terms in the static (non-exchange) potential matrix elements. (These terms are given by Omidvar (1964).) For large L, the incident electron passes by the target atom at a considerable distance. Hence, if L is large enough the

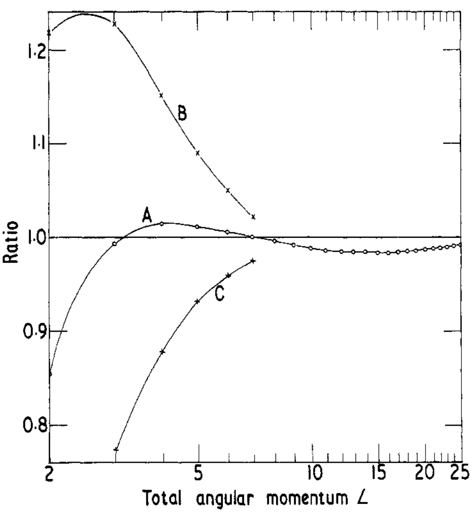

Figure 2. Ratio of imaginary part of the T-matrix element $T^L_{1sL,2pL+1}$ at 54·4 eV calculated using the unitarized Born approximation to the imaginary part of $T^L_{1sL,2pL+1}$ calculated using (A) the 1s–2s–2p close-coupling approximation without exchange and the 1s–2s–2p close-coupling approximation with exchange, singlet (B) and triplet (C).

short-range exponential potentials which appear in the static potentials of Omidvar (1964) can be neglected. The static potentials involving transitions $1s \rightarrow 1s$, $1s \rightarrow 2s$ and $2s \rightarrow 2s$ are short-range potentials of exponential nature and therefore are very small when compared with other transitions. Hence in this paper we put $R^L_{1sL,1sL} = 0$, $R^L_{1sL,2sL} = 0$ and $R^L_{2sL,2sL} = 0$ for large L

The differential cross sections are calculated using the program of Moores (1971).

In figure 2 we plot the ratio of the imaginary part of the T-matrix element $T^L_{1sL,2pL+1}$ at 54·4 eV obtained from the unitarized Born approximation to that obtained from the close-coupling approximation without exchange. It is clear that at large values of L the close-coupling results tend to the unitarized Born calculations and in our calculations it was not difficult to alter the unitarized Born results slightly

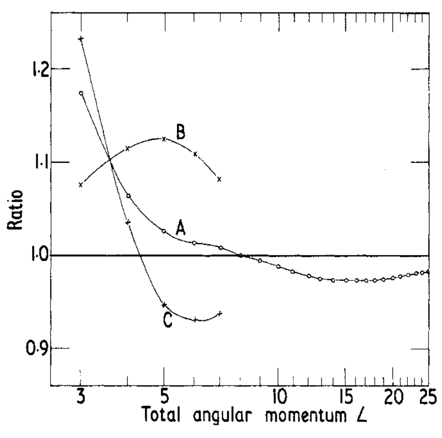

Figure 3. Ratio of the real part of the T-matrix element $T^L_{1sL,2sL}$ at 54·4 eV calculated using the unitarized Born approximation to the real part of $T^L_{1sL,2sL}$ calculated using (A) the 1s–2s–2p close-coupling approximation without exchange and the 1s–2s–2p close-coupling approximation with exchange, singlet (B) and triplet (C).

so that they joined smoothly onto the close-coupling results without exchange. This figure also shows that the close-coupling results with exchange tend to the close-coupling results without exchange and we modified the non-exchange results so that they joined smoothly to the exchange results.

Figure 3 also gives the ratio of the real part of the *T*-matrix element $T^L_{1sL,2sL}$ at 54·4 eV obtained from the unitarized Born approximation to that obtained from the close-coupling approximations.

3. Results and discussion

In presenting our results it is convenient to consider separately the results for incident energies above 54 eV and those below 54 eV. For energies above 54 eV, we expect that the present calculations would not differ appreciably from the exact results. Below 54 eV the scattering process is more complicated and it is known that the 1s–2s–2p close-coupling approximation overestimates the 1s→2s and 1s→2p total excitation cross sections.

3.1. Differential cross sections for $E \geqslant 54$ eV

Tables 2 and 3 contain the differential cross sections for excitation of the 2s and 2p states of hydrogen calculated using the 1s–2s–2p close-coupling approximation†. For both transitions the differential cross section is sharply peaked in the forward direction but decreases slowly at large angles of scattering. At high energies the difference between the magnitude of the forward scattering cross section and the

Table 2. Differential cross section ($a_0^2\text{sr}^{-1}$) for 1s→2s calculated using 1s–2s–2p close-coupling approximation.

Scattering angle θ \ k^2	4·00	7·35	10·00	14·71	22·06
0	3·26	3·57	3·53	3·33	3·46
10	$5{\cdot}75^{-1}$‡	$3{\cdot}65^{-1}$	$3{\cdot}18^{-1}$	$2{\cdot}57^{-1}$	$1{\cdot}77^{-1}$
20	$1{\cdot}23^{-1}$	$8{\cdot}81^{-2}$	$5{\cdot}87^{-2}$	$2{\cdot}78^{-2}$	$1{\cdot}00^{-2}$
30	$4{\cdot}43^{-2}$	$2{\cdot}00^{-2}$	$1{\cdot}07^{-2}$	$4{\cdot}22^{-3}$	$1{\cdot}45^{-3}$
40	$1{\cdot}90^{-2}$	$7{\cdot}59^{-3}$	$3{\cdot}96^{-3}$	$1{\cdot}56^{-3}$	$5{\cdot}23^{-4}$
50	$1{\cdot}24^{-2}$	$4{\cdot}33^{-3}$	$2{\cdot}09^{-3}$	$7{\cdot}55^{-4}$	$2{\cdot}38^{-4}$
60	$9{\cdot}93^{-3}$	$2{\cdot}74^{-3}$	$1{\cdot}22^{-3}$	$4{\cdot}11^{-4}$	$1{\cdot}25^{-4}$
70	$8{\cdot}18^{-3}$	$1{\cdot}84^{-3}$	$7{\cdot}68^{-4}$	$2{\cdot}50^{-4}$	$7{\cdot}26^{-5}$
80	$6{\cdot}66^{-3}$	$1{\cdot}28^{-3}$	$5{\cdot}17^{-4}$	$1{\cdot}61^{-4}$	$4{\cdot}70^{-5}$
90	$5{\cdot}37^{-3}$	$9{\cdot}28^{-4}$	$3{\cdot}63^{-4}$	$1{\cdot}11^{-4}$	$3{\cdot}16^{-5}$
100	$4{\cdot}42^{-3}$	$7{\cdot}05^{-4}$	$2{\cdot}67^{-4}$	$8{\cdot}02^{-5}$	$2{\cdot}26^{-5}$
120	$3{\cdot}31^{-3}$	$4{\cdot}70^{-4}$	$1{\cdot}75^{-4}$	$5{\cdot}14^{-5}$	$1{\cdot}38^{-5}$
140	$2{\cdot}75^{-3}$	$3{\cdot}62^{-4}$	$1{\cdot}32^{-4}$	$3{\cdot}82^{-5}$	$9{\cdot}84^{-6}$
160	$2{\cdot}49^{-3}$	$3{\cdot}11^{-4}$	$1{\cdot}13^{-4}$	$3{\cdot}27^{-5}$	$7{\cdot}74^{-6}$
180	$2{\cdot}41^{-3}$	$3{\cdot}00^{-4}$	$1{\cdot}13^{-4}$	$3{\cdot}2^{-5}$	

† Tables containing the real and imaginary parts of the singlet and triplet scattering amplitudes can be obtained on request from the authors.

‡ Superscript denotes the power of 10 by which the number should be multiplied.

Table 3. Differential cross section ($a_0^2\,sr^{-1}$) for $1s \rightarrow 2p$ calculated using 1s–2s–2p close-coupling approximation.

Scattering angle θ \ k^2	4·00	7·35	10·00	14·71	22·06
0	$3{\cdot}90^{1}$†	$8{\cdot}86^{1}$	$1{\cdot}29^{2}$	$2{\cdot}01^{2}$	$3{\cdot}17^{2}$
10	7·81	4·60	3·02	1·57	$6{\cdot}70^{-1}$
20	1·18	$3{\cdot}22^{-1}$	$1{\cdot}36^{-1}$	$3{\cdot}78^{-2}$	$7{\cdot}82^{-3}$
30	$1{\cdot}99^{-1}$	$3{\cdot}00^{-2}$	$9{\cdot}84^{-3}$	$2{\cdot}39^{-3}$	$5{\cdot}59^{-4}$
40	$4{\cdot}71^{-2}$	$6{\cdot}35^{-3}$	$2{\cdot}37^{-3}$	$6{\cdot}72^{-4}$	$1{\cdot}88^{-4}$
50	$1{\cdot}95^{-2}$	$2{\cdot}73^{-3}$	$1{\cdot}11^{-3}$	$3{\cdot}25^{-4}$	$9{\cdot}76^{-5}$
60	$1{\cdot}11^{-2}$	$1{\cdot}54^{-3}$	$6{\cdot}50^{-4}$	$1{\cdot}93^{-4}$	$6{\cdot}06^{-5}$
70	$6{\cdot}88^{-3}$	$1{\cdot}01^{-3}$	$4{\cdot}30^{-4}$	$1{\cdot}30^{-4}$	$4{\cdot}17^{-5}$
80	$4{\cdot}66^{-3}$	$7{\cdot}35^{-4}$	$3{\cdot}13^{-4}$	$9{\cdot}48^{-5}$	$2{\cdot}98^{-5}$
90	$3{\cdot}38^{-3}$	$5{\cdot}77^{-4}$	$2{\cdot}39^{-4}$	$7{\cdot}53^{-5}$	$2{\cdot}40^{-5}$
100	$2{\cdot}56^{-3}$	$4{\cdot}74^{-4}$	$1{\cdot}91^{-4}$	$6{\cdot}43^{-5}$	$2{\cdot}08^{-5}$
120	$1{\cdot}69^{-3}$	$3{\cdot}50^{-4}$	$1{\cdot}31^{-4}$	$4{\cdot}79^{-5}$	$1{\cdot}36^{-5}$
140	$1{\cdot}31^{-3}$	$2{\cdot}80^{-4}$	$1{\cdot}01^{-4}$	$4{\cdot}10^{-5}$	$1{\cdot}16^{-5}$
160	$1{\cdot}12^{-3}$	$2{\cdot}43^{-4}$	$8{\cdot}50^{-5}$	$3{\cdot}65^{-5}$	$8{\cdot}99^{-6}$
180	$1{\cdot}09^{-3}$	$2{\cdot}34^{-4}$	$8{\cdot}2^{-5}$	$3{\cdot}3^{-5}$	—

† Superscript denotes the power of 10 by which the number should be multiplied.

backward scattering cross section increases rapidly and large cancellation begins to arise, for backward scattering, between two nearly equal positive and negative terms in the partial wave expansion of the scattering amplitudes. This cancellation reduces the accuracy of our calculations at large angles and high energies.

Figure 4 compares our close-coupling results with the Born approximation results at 100 eV. For excitation to both the 2s and 2p states the Born results are several orders of magnitude smaller than the close-coupling results.

It is also interesting to note that in our calculations at large angle scattering the differential cross sections for excitation to the 2s and 2p states are almost equal. In the simple Born approximation the 2s differential cross section may be an order of magnitude larger than the 2p differential cross section (see figure 4). This result clearly comes from the degenerate r^{-2} potential coupling the 2s and 2p channels.

Calculations have also been carried out using the unitarized Born approximation by putting $L_{ee} = L_{ee}^{NE} = 0$. Results of these calculations are given in tables 4 and 5. Figure 4 demonstrates that for excitation to both the 2s and 2p states the unitarized Born approximation gives differential cross sections which are much better than the Born results particularly at large angles of scattering.

The sum of the differential cross sections for excitation of the 2s and 2p states are displayed in figure 5. These functions decrease monotonically as the angle increases. At a fixed angle the cross sections are approximately proportional to E^{-3} at large angles of scattering over the energy range considered here.

The differential cross section for excitation of the 2s and 2p states of hydrogen has been the subject of many previous theoretical investigations. Figure 1 compares a selection of these calculations with the present calculations at 54 eV. Also plotted on this figure are the absolute measurements of Williams and Willis (1975). The present results are in quite good agreement with experiment and are closer to the measurements than any of the earlier calculations.

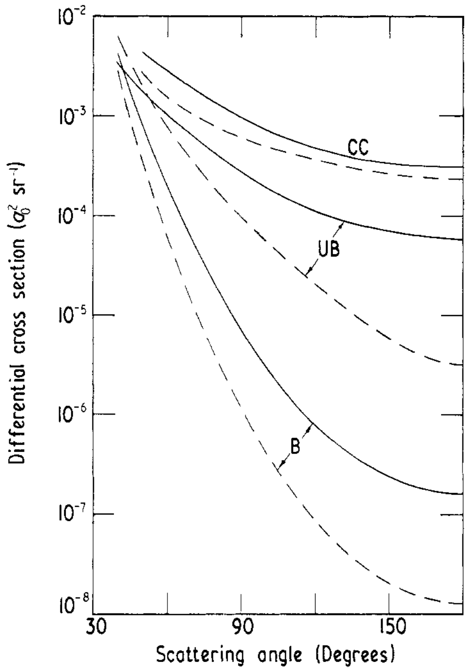

Figure 4. Differential cross section at 100 eV. for excitation of the 2s state (full curve); and excitation of the 2p state (broken curve). Differential cross sections calculated using the Born approximation are denoted by B, those calculated using the unitarized Born approximation by UB and the present close-coupling calculations by CC.

Table 4. Differential cross section (a_0^2sr^{-1}) for 1s$\rightarrow$2s calculated using the unitarized Born approximation.

Scattering angle θ \ k^2	1·00	1·44	2·25	4·00	10·00	14·71	22·06
0	4·43^{-1}†	1·28	2·29	3·18	3·49	3·34	3·08
10	3·55^{-1}	7·91^{-1}	8·56^{-1}	5·24^{-1}	2·86^{-1}	2·30^{-1}	1·59^{-1}
20	1·83^{-1}	2·16^{-1}	1·22^{-1}	9·25^{-2}	4·47^{-2}	2·14^{-2}	7·69^{-3}
30	5·97^{-2}	3·34^{-2}	2·88^{-2}	2·96^{-2}	6·53^{-3}	2·53^{-3}	9·07^{-4}
40	1·02^{-2}	6·65^{-3}	1·38^{-2}	1·01^{-2}	1·85^{-3}	8·02^{-4}	3·11^{-4}
50	4·66^{-3}	4·79^{-3}	7·56^{-3}	4·50^{-3}	8·94^{-4}	3·79^{-4}	1·40^{-4}
60	1·33^{-3}	3·94^{-3}	4·87^{-3}	2·78^{-3}	5·02^{-4}	2·01^{-4}	7·10^{-5}
70	2·12^{-3}	3·36^{-3}	3·82^{-3}	1·99^{-3}	3·00^{-4}	1·15^{-4}	3·98^{-5}
80	1·68^{-3}	3·31^{-3}	3·35^{-3}	1·47^{-3}	1·90^{-4}	7·12^{-5}	2·43^{-5}
90	1·13^{-3}	3·55^{-3}	3·01^{-3}	1·09^{-3}	1·27^{-4}	4·69^{-5}	1·59^{-5}
100	1·24^{-3}	3·89^{-3}	2·68^{-3}	8·18^{-4}	8·92^{-5}	3·28^{-5}	1·12^{-5}
120	4·00^{-3}	4·56^{-3}	2·01^{-3}	5·00^{-4}	5·12^{-5}	1·88^{-5}	6·42^{-6}
140	8·95^{-3}	5·17^{-3}	1·50^{-3}	3·50^{-4}	3·51^{-5}	1·29^{-5}	4·44^{-6}
160	1·36^{-2}	5·67^{-3}	1·20^{-3}	2·84^{-4}	2·81^{-5}	1·04^{-5}	3·59^{-6}
180	1·56^{-2}	5·87^{-3}	1·11^{-3}	2·65^{-4}	2·61^{-5}	9·64^{-6}	3·34^{-6}

† Superscript denotes the power of 10 by which the number should be multiplied.

Table 5. Differential cross section ($a_0^2 \mathrm{sr}^{-1}$) for 1s→2p calculated using the unitarized Born approximation.

Scattering angle θ \ k^2	1·00	1·44	2·25	4·00	10·00	14·71	22·06
0	1·67	6·47	$1{\cdot}75^{1}$	$4{\cdot}40^{1}$	$1{\cdot}39^{2}$	$2{\cdot}13^{2}$	$3{\cdot}29^{2}$
10	1·40	4·42	7·75	7·75	2·96	1·55	$6{\cdot}70^{-1}$
20	$8{\cdot}54^{-1}$†	1·81	1·91	1·06	$1{\cdot}44^{-1}$	$4{\cdot}29^{-2}$	$9{\cdot}70^{-3}$
30	$4{\cdot}15^{-1}$	$6{\cdot}62^{-1}$	$5{\cdot}31^{-1}$	$1{\cdot}94^{-1}$	$1{\cdot}19^{-2}$	$2{\cdot}90^{-3}$	$6{\cdot}47^{-4}$
40	$1{\cdot}88^{-1}$	$2{\cdot}77^{-1}$	$1{\cdot}81^{-1}$	$4{\cdot}57^{-2}$	$2{\cdot}20^{-3}$	$5{\cdot}82^{-4}$	$1{\cdot}44^{-4}$
50	$9{\cdot}90^{-2}$	$1{\cdot}40^{-1}$	$7{\cdot}13^{-2}$	$1{\cdot}42^{-2}$	$6{\cdot}96^{-4}$	$1{\cdot}91^{-4}$	$4{\cdot}79^{-5}$
60	$6{\cdot}74^{-2}$	$7{\cdot}86^{-2}$	$3{\cdot}14^{-2}$	$5{\cdot}61^{-3}$	$2{\cdot}79^{-4}$	$7{\cdot}75^{-5}$	$1{\cdot}95^{-5}$
70	$5{\cdot}28^{-2}$	$4{\cdot}57^{-2}$	$1{\cdot}54^{-2}$	$2{\cdot}56^{-3}$	$1{\cdot}28^{-4}$	$3{\cdot}59^{-5}$	$9{\cdot}08^{-6}$
80	$4{\cdot}18^{-2}$	$2{\cdot}75^{-2}$	$8{\cdot}29^{-3}$	$1{\cdot}27^{-3}$	$6{\cdot}46^{-5}$	$1{\cdot}83^{-5}$	$4{\cdot}67^{-6}$
90	$3{\cdot}23^{-2}$	$1{\cdot}74^{-2}$	$4{\cdot}75^{-3}$	$6{\cdot}61^{-4}$	$3{\cdot}51^{-5}$	$9{\cdot}99^{-6}$	$2{\cdot}58^{-6}$
100	$2{\cdot}50^{-2}$	$1{\cdot}18^{-2}$	$2{\cdot}82^{-3}$	$3{\cdot}63^{-4}$	$2{\cdot}01^{-5}$	$5{\cdot}76^{-6}$	$1{\cdot}51^{-6}$
120	$1{\cdot}84^{-2}$	$6{\cdot}60^{-3}$	$1{\cdot}06^{-3}$	$1{\cdot}28^{-4}$	$7{\cdot}50^{-6}$	$2{\cdot}14^{-6}$	$5{\cdot}64^{-7}$
140	$2{\cdot}00^{-2}$	$4{\cdot}36^{-3}$	$4{\cdot}34^{-4}$	$5{\cdot}58^{-5}$	$3{\cdot}14^{-6}$	$8{\cdot}85^{-7}$	$2{\cdot}26^{-7}$
160	$2{\cdot}43^{-2}$	$3{\cdot}31^{-3}$	$2{\cdot}21^{-4}$	$3{\cdot}12^{-5}$	$1{\cdot}53^{-6}$	$4{\cdot}18^{-7}$	$1{\cdot}01^{-7}$
180	$2{\cdot}64^{-2}$	$3{\cdot}00^{-3}$	$1{\cdot}71^{-4}$	$2{\cdot}51^{-5}$	$1{\cdot}13^{-6}$	$3{\cdot}2^{-7}$	

† Superscript denotes the power of 10 by which the number should be multiplied.

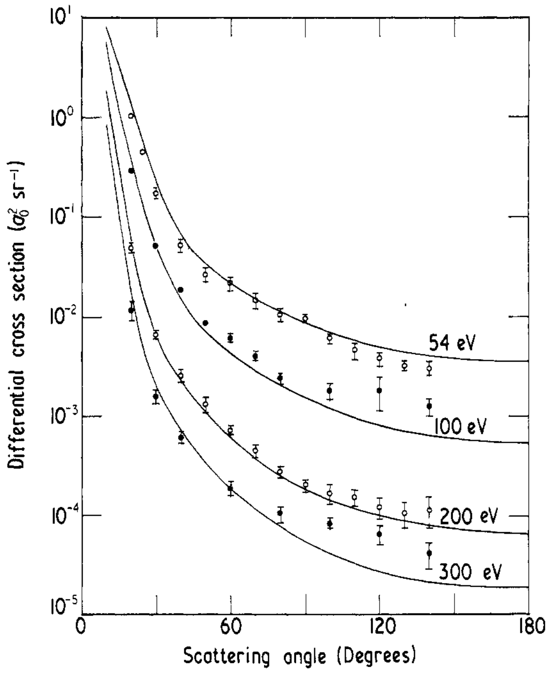

Figure 5. Differential cross section for e + H(1s) → e + H(2s + 2p) at 54, 100, 200 and 300 eV. Full curve, present 1s–2s–2p close-coupling approximation calculations; experimental measurements (open and full symbols with error bars) by Williams and Willis (1975).

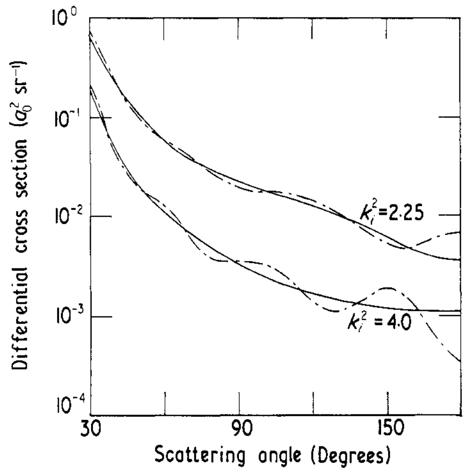

Figure 6. Differential cross section for the process e + H(1s) → e + H(2p) at 2·25 and 4·0 Ryd. Full curve, present 1s–2s–2p close-coupling calculation; broken curve, calculations by Brandt and Truhlar (1975).

The calculations of Scott (1965) and Brandt and Truhlar (1975) (see figure 6) both give differential cross sections which have small oscillations. Our calculations did not have these oscillations; however we could obtain similar oscillations either by the introduction of small errors in our R matrices or by using a very small number of partial waves.

In figure 5 we also compare our calculations with the measurements of Williams and Willis (1975). Although the agreement between theory and experiment is quite good there is a significant difference between the calculations and the measurements at large angles of scattering for incident energies of 100 and 300 eV.

3.2. *Differential cross sections for 13 eV < E < 54 eV*

It is more difficult to describe the scattering process in this energy range. Effects due to other channels must become important as the energy decreases towards the ionization threshold. The total cross sections for excitation from the ground state to the $n = 2$ states calculated by Burke *et al* (1963) using the 1s–2s–2p close-coupling approximation are too large when compared with normalized relative measurements (see Moiseiwitsch and Smith 1968) and thus we do not expect the 1s–2s–2p close-coupling approximation to be reliable in this energy range. However, in the absence of reliable absolute measurements, the present differential cross section calculations should provide us with some indication of the shape and qualitative features of the cross section curves. In addition they will provide a standard against which later more accurate calculations can be judged.

Figures 7 and 8 display the differential cross sections for excitation of the 2s and 2p states of hydrogen calculated using the 1s–2s–2p close-coupling approximation. The pattern of the results is quite complex. The most distinctive feature is the sharp dip which arises in the 1s → 2s differential cross section for energies between 1 and 2·25 Ryd. The dip occurs because the scattering amplitude which dominates this differential cross section changes sign near this minimum. The differential cross section does not however become zero because of the contributions from the other scattering

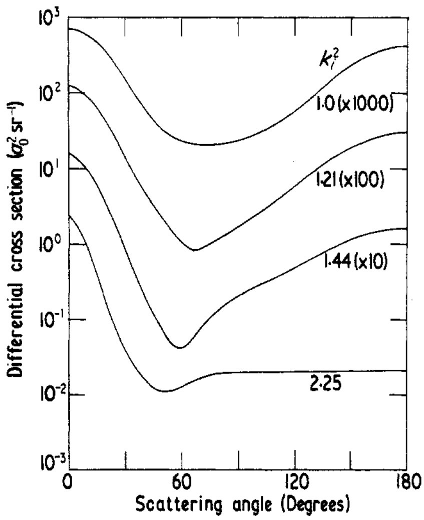

Figure 7. Differential cross section for e + H(1s) → e + H(2s) at 1·00, 1·21, 1·44 and 2·25 Ryd calculated using the 1s–2s–2p close-coupling approximation.

amplitudes. This pattern also arises in the electron excitation of the 2^1S state of helium (Trajmar 1973).

3.3. *Total cross sections*

The total cross sections for excitation of the 2s and 2p states have also been calculated using the 1s–2s–2p close-coupling approximation; these are presented in tables 6 and 7. These close-coupling results are compared with Born and unitarized Born calculations and also with earlier 1s–2s–2p close-coupling results obtained by Burke *et al* (1962) for energies below 54 eV. In most cases only a marginal difference is

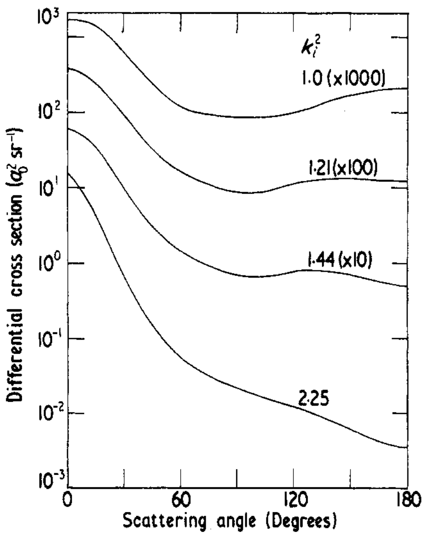

Figure 8. Differential cross section for e + H(1s) → e + H(2p) at 1·00, 1·21, 1·44 and 2·25 Ryd calculated using the 1s–2s–2p close-coupling approximation.

Table 6. Calculated total cross section $\sigma^{T}_{1s\to 2s}$ for the process $e + H(1s) \to e + H(2s)$ (πa_0^2).

Energy (Ryd)	1·00	1·21	1·44	2·25	4·00	7·35	10·00	14·71	22·06
Energy (eV)	13·6	16·5	19·6	30·6	54·4	100	136	200	300
1s–2s–2p (present)	$3{\cdot}62^{-1}$†	$3{\cdot}39^{-1}$	$2{\cdot}64^{-1}$	$1{\cdot}60^{-1}$	$1{\cdot}01^{-1}$	$5{\cdot}82^{-2}$	$4{\cdot}36^{-2}$	$3{\cdot}00^{-2}$	$2{\cdot}01^{-2}$
1s–2s–2p (Burke *et al* 1963)	$3{\cdot}62^{-1}$	$3{\cdot}40^{-1}$	$2{\cdot}64^{-1}$	$1{\cdot}60^{-1}$	$1{\cdot}01^{-1}$				
Unitarized Born	$7{\cdot}12^{-2}$	$9{\cdot}40^{-2}$	$1{\cdot}02^{-1}$	$9{\cdot}87^{-2}$	$7{\cdot}44^{-2}$	$4{\cdot}82^{-2}$	$3{\cdot}76^{-2}$	$2{\cdot}69^{-2}$	$1{\cdot}87^{-2}$
Born	$2{\cdot}48^{-1}$	$2{\cdot}46^{-1}$	$2{\cdot}28^{-1}$	$1{\cdot}67^{-1}$	$1{\cdot}02^{-1}$	$5{\cdot}77^{-2}$	$4{\cdot}30^{-2}$	$2{\cdot}95^{-2}$	$1{\cdot}98^{-2}$

† Superscript denotes the power of 10 by which the number should be multiplied.

Table 7. Calculated total cross section $\sigma^{T}_{1s\to 2p}$ for the process $e + H(1s) \to e + H(2p)$ (πa_0^2).

Energy (Ryd)	1·00	1·21	1·44	2·25	4·00	7·35	10·00	14·71	22·06
Energy (eV)	13·6	16·5	19·6	30·6	54·4	100	136	200	300
1s–2s–2p (present)	$8{\cdot}00^{-1}$†	1·08	1·18	1·10	$9{\cdot}08^{-1}$	$6{\cdot}81^{-1}$	$5{\cdot}73^{-1}$	$4{\cdot}52^{-1}$	$3{\cdot}46^{-1}$
1s–2s–2p (Burke *et al* 1963)	$8{\cdot}00^{-1}$	1·09	1·18	1·09	$8{\cdot}72^{-1}$				
Unitarized Born	$4{\cdot}39^{-1}$	$6{\cdot}56^{-1}$	$8{\cdot}01^{-1}$	$9{\cdot}73^{-1}$	$9{\cdot}08^{-1}$	$7{\cdot}02^{-1}$	$5{\cdot}92^{-1}$	$4{\cdot}66^{-1}$	$3{\cdot}54^{-1}$
Born	1·04	1·23	1·31	1·28	1·04	$7{\cdot}50^{-1}$	$6{\cdot}20^{-1}$	$4{\cdot}80^{-1}$	$3{\cdot}61^{-1}$

† Superscript denotes the power of 10 by which the number should be multiplied.

noted between the present close-coupling calculations and the earlier close-coupling results. However a 4% difference is observed between these two calculations for the total cross section, $\sigma^{T}_{1s\to 2p}$, for excitation of the 2p state at 54 eV. This discrepancy is partly due to the larger number of partial waves used in the present calculations and partly due to the fact that the contribution from the higher partial waves are now obtained from the unitarized Born approximation instead of the Born approximation.

Table 6 shows that for the total cross section for excitation to the 2s state the 1s–2s–2p close-coupling approximation gives results which are about 1·5% larger than the cross section given by the Born approximation for incident electron energies between 150 and 300 eV. For excitation to the 2p state the Born cross section is about 15% larger than the close-coupling cross section at 54 eV but at 300 eV the cross sections given by the two approximations only differ by about 4%. Damburg and Propin (1972) have suggested that at electron energies from 200 eV to 1000 eV the effect of 2s–2p degenerate channel coupling may give cross sections for excitation of the 2p state which differ from the Born approximation by 20%. Our close-coupling results show that 2s–2p coupling produces a much smaller effect than that predicted by Damburg and Propin.

At large impact energies the Born approximation gives a 2s excitation cross section which is closer to the close-coupling cross section than the excitation cross section given by the unitarized Born approximation. For excitation of the 2p state the unitarized Born approximation cross section lies closer to the close-coupling cross section than the Born approximation cross section.

4. Conclusion

There is quite good agreement between the measured differential cross section for excitation of the $n = 2$ states of hydrogen (Williams and Willis 1975) and the present 1s–2s–2p close-coupling calculations for incident electron energies above 54 eV. This indicates that the 1s–2s–2p close-coupling approximation may be sufficient to describe the scattering process above 54 eV. Further experimental work is needed to clarify the situation above 54 eV. Below 54 eV the 1s–2s–2p close-coupling approximation does not describe the scattering process and further calculations which include pseudostates are at present in progress for this energy region. Similar calculations have been carried out by Callaway *et al* (1975).

Acknowledgments

This research was accomplished with the support of the US Office of Naval Research under Contract N00014-69-C-0035. Part of the computer time was granted by the Science Research Council at the Atlas Computer Laboratory. The authors are grateful to Dr J F Williams for supplying his results prior to publication. One of us (WCF) would like to acknowledge his gratitude to the Department of Applied Mathematics and Theoretical Physics, The Queen's University of Belfast, Northern Ireland, for the award of a Postdoctoral Fellowship.

References

Brandt M A and Truhlar D G 1975 *Phys. Rev.* **11** 1340–6
Bransden B N, Coleman J P and Sullivan J 1972 *J. Phys. B: Atom. Molec. Phys.* **5** 546–58
Burke P G 1972 *Atoms and Molecules in Astrophysics, Proc. Scottish Universities Summer School, Stirling, 1971* ed T R Carson and M J Roberts (London: Academic Press) pp 1–63
Burke P G and Schey H M 1962 *Phys. Rev.* **126** 147–62
Burke P G, Schey H M and Smith K 1963 *Phys. Rev.* **129** 1258–74
Burke P G and Smith K 1962 *Rev. Mod. Phys.* **34** 458–502
Callaway J, McDowell M R C and Morgan L A 1975 *Proc. 9th Int. Conf. on Physics of Electronic and Atomic Collisions, Seattle* ed J S Risley and R Geballe (Seattle and London: University of Washington Press) p 675
Damburg R and Propin R 1972 *J. Phys. B: Atom. Molec. Phys.* **5** 533–6
Geltman S and Hidalgo M H 1971 *J. Phys. B: Atom. Molec. Phys.* **4** 1299–307
Ghosh A S and Sil N C 1970 *Ind. J. Phys.* **44** 153–61
Lawson J, Lawson W and Seaton M J 1961 *Proc. Phys. Soc.* **77** 192–8
McDowell M R C, Morgan L A and Myerscough V P 1975 *J. Phys. B: Atom. Molec. Phys.* **8** 1053–72
Moiseiwitsch B L and Smith S J 1968 *Rev. Mod. Phys.* **40** 238–353
Moores D L 1971 *Comp. Phys. Commun.* **2** 360–7
Omidvar K 1964 *Phys. Rev.* **133** A970–85
Scott B L 1965 *Phys. Rev.* **140** A699–704
Shelton W N, Leherissey E S and Madison D H 1971 *Phys. Rev.* A **3** 242–50
Trajmar S 1973 *Phys. Rev.* A **8** 191–203
Williams K L 1969 *Proc. 6th Int. Conf. on Physics of Electronic and Atomic Collisions, Boston* (Cambridge, Mass: MIT Press) pp 731–4
Williams J F and Willis B A 1974 *J. Phys. B: Atom. Molec. Phys.* **7** L61–5
—— 1975 *J. Phys. B: Atom. Molec. Phys.* **8** 1641–69